Preparation and photoabsorption characterization of $BiFeO_3$ nanowires

F. Gao, Y. Yuan, K. F. Wang, X. Y. Chen, F. Chen, and J.-M. Liu[a)]
Laboratory of Solid State Microstructures, Nanjing University, Nanjing 210093, China and International Center for Materials Physics, Chinese Academy of Sciences, Shenyang 110015, China

Z. F. Ren
Department of Physics, Boston College, Chestnut Hill, Massachusetts 02467 and Laboratory of Solid State Microstructures, Nanjing University, Nanjing 210093, China

(Received 9 March 2006; accepted 16 July 2006; published online 7 September 2006)

Perovskite-type polycrystalline $BiFeO_3$ (BFO) nanowires (~50 nm in diameter and ~5 μm in length) were synthesized using the anodized alumina template technique. An energy band gap of ~2.5 eV was determined from the UV-visible diffuse reflectance spectrum, and its photocatalytic ability to produce O_2 was revealed under UV irradiation. Weak ferromagnetism at room temperature and superparamagnetism at low temperature were observed for the BFO nanowires, different from the antiferromagnetic order in bulk BFO, reflecting the significant size effects on the magnetic ordering of BFO. © *2006 American Institute of Physics*. [DOI: 10.1063/1.2345825]

Nanoscale materials, which are of great fundamental and technological interests, exhibit a wide range of magnetic,[1] electrical, and optical properties[2] as a result of their low dimensionality and quantum confinement effect. Among them, oxide nanowires have shown a variety of interesting properties that make them useful for a wide range of applications including catalysts, magnetic devices, and sensors.[1] Even though a variety of methods have been used for fabrication of nanowires, the template approach has been widely employed. Possible templates include nuclear track-etched polycarbonate membranes, nanochannel array glasses, mesoporous channel hosts, and self-ordered anodized aluminum oxide (AAO) films. AAO template with pore diameters of 10–200 nm remains stable at high temperature and in organic solvents, and the pores are uniform in size and well aligned perpendicular to the membrane surface. These advantages make AAO templates ideal for the synthesis of oxide nanowires.[2]

The synthesis of multiferroic nanostructures with a controllable size and shape is essential not only for new device applications but also for fundamental studies.[3] Among all the multiferroic materials studied so far, $BiFeO_3$ (BFO) that exhibits the coexistence of ferroelectric (FE) and antiferromagnetic (AFM) orders has received great attention,[4–6] due to its high FE Curie point[7] ($T_C \sim 1103$ K) and the AFM Néel point ($T_N \sim 647$ K).[8] The AFM spin order in BFO ceramics is spatially modulated, resulting in no macroscopic magnetization at room temperature (RT).[4] Interestingly, weak ferromagnetic (FM) order was observed in BFO films at RT, allowing them to be one of the prime candidates for RT magnetoelectric applications.[5,6] Although the origin of the FM order in BFO films is not clear, the underlying physics is probably associated with the low dimensionality (size effect), allowing relaxation of the spatially modulated AFM order to some extent. BFO nanostructures, potentially useful for future applications, such as vertical magnetic recording with ultrahigh recording density, provide an additional degree of freedom for spin relaxation due to the size effect, making it possible for a weak FM ordering. Furthermore, Bi-contained perovskite oxides often offer interesting optical properties for photocatalytic applications.[9,10] It would be interesting to explore any possibility of BFO as photocatalyst. Although there are reports on the preparation and electric properties of BFO nanotubes,[3,11] neither any data on the magnetic properties of BFO nanostructures nor their optical properties for photocatalytic applications are available. In this letter, we report the synthesis of BFO nanowires by sol-gel template technique and the characterization of the magnetic and optical performances.

About 5 μm thick AAO templates with a pore diameter of ~50 nm were prepared by means of anodization.[12] Bismuth nitrate $[Bi(NO_3)_3 \cdot 5H_2O]$ and iron nitrate $[Fe(NO_3)_3 \cdot 9H_2O]$ in stoichiometric proportions (1:1 mole ratio) were dissolved in 2-methoxyethanol ($C_3H_8O_2$), followed by stirring the mixture for about half an hour at RT. The concentration of the final solution was adjusted to 0.3*M* with a *p*H value of 4–5 by adding 2-methoxyethanol and nitric acid. The AAO templates were immersed in the solution for 12 h. In order to obtain the perovskite-type nanowires, the filled templates were heat treated in air at 750 °C for 1 h and then immersed in a 4*M* NaOH solution for 12 h to free the BFO nanowires. The final products were collected and washed thoroughly with de-ionized water.

The crystallinity and morphology of the BFO nanowires were examined by x-ray diffraction (XRD), scanning electron microscopy (SEM), and transmission electron microscopy (TEM). Thermogravimetric analysis (TGA) and differential scanning calorimetric (DSC) analysis were carried out over the temperature range of 300–900 °C in nitrogen ambient to study the FE phase transitions. The heating rate was kept at 10 °C/min. The UV-visible diffuse reflectance spectrum of the nanowires was measured using the UV-visible spectrometry. A superconducting quantum interference device (SQUID) magnetometer was employed to characterize the magnetization (M) as a function of temperature (T) and magnetic field (H).

Figure 1(a) shows the SEM image of our BFO nanowires randomly deposited onto a silicon substrate. These nanowires have almost identical diameter of ~50 nm. All of

[a)]Author to whom correspondence should be addressed; electronic mail: liujm@nju.edu.cn

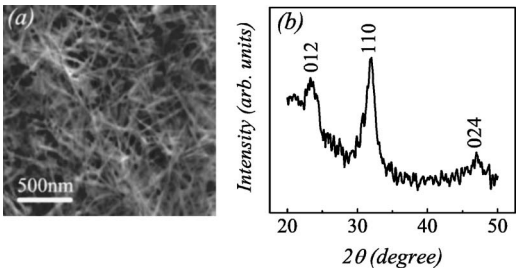

FIG. 1. (a) SEM image and (b) XRD pattern of the BFO nanowires prepared using the sol-gel AAO template method.

the reflections in the XRD spectrum shown in Fig. 1(b) can be indexed according to the lattice structure of bulk BFO. No observable second phases were detected. The broad XRD reflections are ascribed to the small diameters of the nanowires.[13] The crystallinity and morphology of a single BFO nanowire of ~50 nm in diameter and 5 μm in length were analyzed by TEM and are shown in Fig. 2(a), in good agreement with the pore diameters of the AAO templates. The inset shows a selected area electron diffraction (SAED) pattern taken from the nanowire, revealing the polycrystalline nature. The BFO structure was further confirmed by the high-resolution TEM image where the interplanar spacing is 0.28 nm, corresponding to the (110) plane.

The measured TGA and DSC curves of the BFO nanowires are shown in Fig. 3(a). Because the TGA plot remains constant over the whole T range, the distinct endothermic anomaly at ~834 °C in the DSC plot is ascribed to the FE phase transition, noting the Curie point $T_C \sim 1103$ K, as identified in BFO single crystal using polarized light microscopy.[7] In addition, a similar anomaly in the differential thermal analyzer curve of pure BFO ceramic was reported by Kumar *et al.*[14] Therefore, the FE transition point of the BFO nanowires seems not very different from the bulk BFO.

Photocatalytic performances of BFO nanowires were examined in various conditions. Details of the experimental procedure were described elsewhere.[15] Figure 3(b) shows the UV-visible optical absorption behaviors of the as-prepared BFO nanowires. According to the UV-visible diffuse reflectance spectrum, BFO nanowires has an absorption edge at around 490 nm and its energy band gap, estimated from $(\alpha h\nu)^2 - h\nu$ plot,[16] is about 2.5 eV, consistent with previous report.[17] We found that BFO nanowires failed to produce H_2 either from pure water or from $Pt/CH_3OH/H_2O$ solution under visible light irradiation and UV irradiation, which was consistent with the results on BFO nanoparticles.[18] This shows that though BFO has a suitable band gap, its photo induced reduction ability is poor and the reason is being

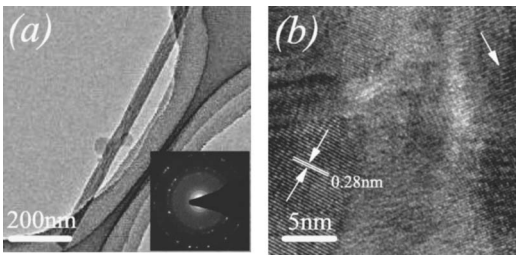

FIG. 2. (a) TEM image of an isolated BFO nanowire with the SAED pattern in the inset; (b) high-resolution TEM image of the nanowire.

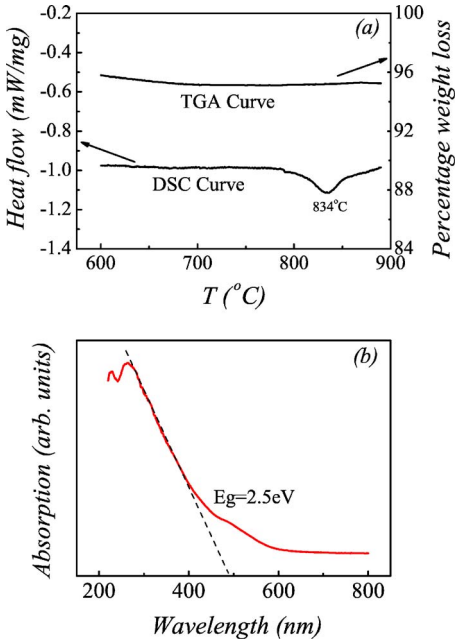

FIG. 3. (a) DSC and TGA curves for the BFO nanowires over 600–890 °C; (b) UV-visible diffuse reflectance spectrum of the BFO nanowires.

further studied. However, in our experiment, BFO nanowires showed the photoinduced oxidization ability to produce O_2 in $AgNO_3/H_2O$ system with considerable initial efficiency of 1876.28 μmol $h^{-1}g^{-1}$. This indicates that BFO would be a good candidate as a photoelectrode as well as a photocatalytic decomposition material. In addition, considering the fact that $SrTiO_3$ coated BFO nanoparticles can produce H_2,[18] our result implies that BFO based materials might have the possibility to produce H_2 and O_2 simultaneously.

The magnetic measurements on the BFO nanowires were performed in order to investigate the magnetic ordering at different temperatures. It is necessary to point out that the BFO nanowires for the measurements were random and the data represent the average of all orientations. As shown in Fig. 4(a), BFO nanowires show a weak FM order at RT, similar to BFO films[6] but different from the linear M-H relationship in bulk BFO.[4] Although the FM origin in BFO films is still a question under debate, it was once suggested that epitaxial strain and oxygen vacancies associated with Fe^{2+} ions in the films contribute to the magnetization.[19] However, Eerenstein *et al.* reported a M of $\sim 0.04\mu_B$/Fe in BFO films without Fe^{2+}, which is independent of the epitaxial strain.[6] It may be argued that the weak FM order in BFO films may be ascribed to the size effect. It is interesting to note that the saturated M at RT for the BFO nanowires is $\sim 0.03\mu_B$/Fe, comparable with the value of BFO films.[6] Although the present work does not present direct evidence with the size effect on the magnetic order, one may be reminded the fact that the wavelength of the incommensurate cycloid spin structure of BFO is 62 nm (Ref. 20) and our nanowires are ~50 nm in diameter. We argue that the cycloid structure of bulk BFO was partially destroyed in the BFO nanowires, which contributes to the weak FM behaviors at RT. At much lower temperature (T=5 K), this size effect will become more significant, evidenced by the M-H loop at T=5 K, as shown in Fig. 4(a). In fact, it was reported that the cycloid structure becomes more anharmonic at lower T and its detrimental effect on the magnetic ordering is

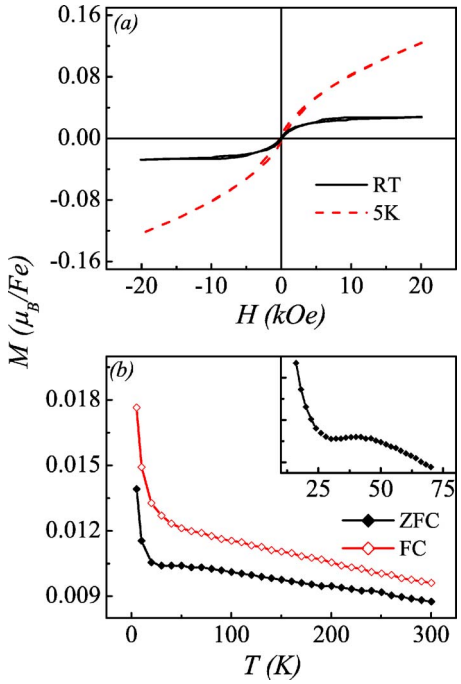

FIG. 4. (a) *M-H* hysteresis loops for the BFO nanowires measured at RT and $T=5$ K. (b) *M-T* curves for the BFO nanowires measured under ZFC and FC ($H=0.1$ T) conditions. The inset presents the ZFC data over a narrower *T* range.

devalued.[20] Therefore, in the BFO nanowires, the spin relaxation from the spatially modulated AFM configuration can be quite significant, resulting in weak FM behaviors and enhanced *M* at low *T*.

In addition, we measured *M* (at $H=100$ Oe) as a function of *T* for the BFO nanowires under zero-field-cooling (ZFC) and 0.1 T field-cooling (FC) conditions, as shown in Fig. 4(b). For the ZFC case, the weak FM state is retained from RT to 42 K, below which a slight decrease in *M* with *T* down to 30 K was observed, as shown more clearly in the inset of Fig. 4(b). When *T* decreases from 30 to 5 K, a rapid increase in *M* was recorded, indicating the superparamagnetic (SPM) behavior. Due to the significant size effect (the large surface/volume ratio) for nanoscale materials, the spin-glass-like surface layer contributes essentially to the sample's magnetization,[21] which will be in a frozen state at very low *T*. In fact, earlier reports on $La_{2/3}Ca_{1/3}MnO_3$ nanodots[22] and Fe nanowires[23] presented a similar SPM behavior at low *T* due to the nanoscale size effect. Upon cooling of the sample under the FC condition, the measured *M* is much higher than the ZFC case, another indication of the SPM state at low *T*. We suggest that, because of the large length-to-diameter ratio ($\sim$100), the effective magnetic field along the wire axis is much larger than that perpendicular to the wire axis. Under the FC condition, the magnetic domains will be directionally ordered to some extent, resulting in the enhanced *M*.

In summary, we have fabricated BFO nanowires, about 5 μm in length and 50 nm in diameter, using a sol-gel AAO template method. The as-prepared polycrystalline nanowires show a perovskite-type structure. The FE phase transition occurs at almost the same temperature as the bulk BFO. The weak ferromagnetism at room temperature is confirmed by the existence of magnetic hysteresis loop. At low temperature, significant superparamagnetic (spin-glass-like) behaviors have been observed. In addition, the photoinduced oxidation ability of BFO nanowires has been revealed, indicating that BFO would be useful in photoelectrode material and photocatalytic decomposition of contamination.

This work was supported by the National Natural Science Foundation of China (50332020, 50528203, 50502018, 10021001, and 20373025) and National Key Projects for Basic Research of China (2002CB613303).

[1] R. Skomski, J. Phys.: Condens. Matter **15**, R841 (2003).
[2] C. R. Martin, Science **266**, 1961 (1994).
[3] X. Y. Zhang, C. W. Lai, X. Zhao, D. Y. Wang, and J. Y. Dai, Appl. Phys. Lett. **87**, 143102 (2005).
[4] S. T. Zhang, M. H. Lu, D. Wu, Y. F. Chen, and N. B. Ming, Appl. Phys. Lett. **87**, 262907 (2005).
[5] J. Wang, J. B. Neaton, H. Zheng, V. Nagarajan, S. B. Ogale, B. Liu, D. Viehland, V. Vaithyanathan, D. G. Schlom, U. V. Waghmare, N. A. Spaldin, K. M. Rabe, M. Wuttig, and R. Ramesh, Science **299**, 1719 (2003).
[6] W. Eerenstein, F. D. Morrison, J. Dho, M. G. Blamire, J. F. Scott, and N. D. Mathur, Science **307**, 1203a (2005).
[7] C. Tabares-Munoz, J. P. Rivera, A. Monnier, and H. Schmid, Jpn. J. Appl. Phys., Suppl. **24**, 1051 (1985).
[8] P. Fischer, M. Polomska, I. Sosnowska, and M. Szymanksi, J. Phys. C **13**, 1931 (1980).
[9] J. W. Tang, Z. G. Zou, and J. H. Ye, Angew. Chem., Int. Ed. **43**, 4463 (2004).
[10] Z. G. Zou, J. H. Ye, and H. Arakawa, Solid State Commun. **119**, 471 (2001).
[11] T. J. Park, Y. B. Mao, and S. S. Wong, Chem. Commun. (Cambridge) **23**, 2708 (2004).
[12] F. Chen, H. W. Liu, K. F. Wang, H. Yu, S. Dong, X. Y. Chen, X. P. Jiang, Z. F. Ren, and J.-M. Liu, J. Phys.: Condens. Matter **17**, L467 (2005).
[13] D. Wu, Y. F. Chen, J. Liu, X. N. Zhao, A. D. Li, and N. B. Ming, Appl. Phys. Lett. **87**, 112501 (2005).
[14] M. M. Kumar, V. R. Palkar, K. Srinivas, and V. Suryanarayana, Appl. Phys. Lett. **76**, 2764 (2000).
[15] Z. G. Zou, J. H. Ye, K. Sayama, and H. Arakawa, J. Photochem. Photobiol., A **148**, 65 (2002).
[16] M. A. Butler, J. Appl. Phys. **48**, 1914 (1977).
[17] T. Takahashi, N. Kida, and M. Tonouchi, Phys. Rev. Lett. **96**, 117402 (2006).
[18] J. Lou and P. A. Maggard, Adv. Mater. (Weinheim, Ger.) **18**, 514 (2006).
[19] J. Wang, A. Scholl, H. Zheng, S. B. Ogale, D. Viehland, D. G. Schlom, N. A. Spaldin, K. M. Rabe, M. Wuttig, L. Mohaddes, J. Neaton, U. Waghmare, T. Zhao, and R. Ramesh, Science **307**, 1203b (2005).
[20] A. V. Zalesskii, A. K. Zvezdin, A. A. Frolov, and A. A. Bush, JETP Lett. **71**, 465 (2000).
[21] R. H. Kodama, S. A. Makhlouf, and A. E. Berkowitz, Phys. Rev. Lett. **79**, 1393 (1997).
[22] P. Katiyar, D. Kumar, T. K. Nath, A. V. Kvit, J. Narayan, S. Chattopadhyay, W. M. Gilmore, S. Coleman, C. B. Lee, J. Sankar, and P. K. Singh, Appl. Phys. Lett. **79**, 1327 (2001).
[23] X. Y. Zhang, G. H. Wen, Y. F. Chan, R. K. Zheng, X. X. Zhang, and N. Wang, Appl. Phys. Lett. **83**, 3341 (2003).